ISSN 1063-7788, Physics of Atomic Nuclei, 2022, Vol. 85, No. 6, pp. 737–747. © Pleiades Publishing, Ltd., 2022.
Russian Text © The Author(s), 2022, published in Yadernaya Fizika, 2022, Vol. 85, No. 6, pp. 490–500.

ELEMENTARY PARTICLES AND FIELDS
Theory

Gluon Sivers Function in Transverse Single-Spin Asymmetries of Direct Photons at NICA

V. A. Saleev[1),2)*] and A. V. Shipilova[1),2)]**

Received May 5, 2022; revised May 5, 2022; accepted June 13, 2022

Abstract—Transverse single-spin asymmetries in the production of direct photons at the Nuclotron-based Ion Collider fAcility (NICA) are studied within the generalized parton model and its color gauge-invariant extension. Predictions for the possible asymmetry values at various NICA energies are presented. A kinematical region where the contribution of the gluon Sivers function to the asymmetry in question is dominant over the quark Sivers function is found.

DOI: 10.1134/S1063778822060114

1. INTRODUCTION

Investigation of transverse single-spin asymmetries in terms of the Sivers function [1] provides the possibility of determining the interrelation between the spin of a transversely polarized nucleon and the intrinsic transverse momentum of quarks and gluons. A precise knowledge of the Sivers function improves substantially our knowledge of the three-dimensional structure of the proton and permits estimating the parton orbital angular momentum [2–5].

For an overview of experimental and theoretical data on transverse single-spin asymmetries, the interested reader is referred to [6, 7]. At the present time, investigation of these asymmetries is an indispensable part of research programs for many future experiments, described, for example, [8, 9], including the SPD experiment at the Nuclotron-based Ion Collider fAcility (NICA) [10], where it is planned to implement proton–proton and proton–deuteron collisions by employing polarized beams of center-of-mass collision energy extending up to $\sqrt{S} = 27$ GeV.

At the present time, there exist two basic theoretical approaches to describing transverse single-spin asymmetries. Of these, one is based on the collinear-factorization mechanism in the next-to-leading order in the hard scale (twist-3), where the single-spin asymmetries are expressed in terms of the convolution of universal nonperturbative quark–gluon–quark correlation functions and hard scattering amplitudes [11–15]. The other [16–20] relies on the generalized parton model (GPM) [21] and involves introducing, within it parton distributions that depend on the transverse momentum of the primary quark or gluon [22]; among them the Sivers distribution function plays a key role for transverse single-spin asymmetries. Its universality (process independence) is violated upon taking into account initial- and final-state interactions (ISI and FSI, respectively) of partons with the spectators of the polarized proton. The effects of ISI and FSI can be taken into account in the approximation of one-gluon exchange within the color gauge-invariant extension of the GPM approach [23–25]. A direct relationship between the GPM and twist-3 approaches was demonstrated in [26–28]; moreover, their equivalence in the intersection of their applicability regions was proven in [29]. Within the GPM approach, a successful phenomenological description of single-spin asymmetries was constructed in a number of studies—in [30–33] for open- and hidden-charm production and in [34, 35] for the production of pions and direct photons.

The quark Sivers function has been studied both experimentally and theoretically (see, for example, [36, 37] and references therein). Much less is known about the gluon Sivers function [38]. In order to study this function, it is advisable to consider hadron–hadron collision processes such in which its contribution is expected to be dominant. They include the process of direct photon production, since it is dominated by the Compton process of quark–gluon scattering. Moreover, a photon does not carry a color charge; therefore, there is no need for introducing a model for describing final-state hadronization and for taking into account FSI effects.

The objective of the present study is to calculate transverse single-spin asymmetries within the GPM approach and to assess the possibility of observing

[1)] Samara National Research University, Samara, Russia.
[2)] Joint Institute for Nuclear Research, Dubna, Russia.
[*] E-mail: saleev@samsu.ru
[**] E-mail: a.v.shipilova@ssau.ru

them in processes of direct photon production in $p^{\uparrow}p$ collisions at the NICA energies.

2. DIRECT-PHOTON PRODUCTION IN THE COLLINEAR PARTON AND GENERALIZED PARTON MODELS

Inclusive photons of high transverse momentum (p_T) may be produced both directly in a hard parton subprocess and as the result of emission from the final parton produced in the hard subprocess. Therefore, we will call them direct photons and fragmentation photons, respectively.

In the leading order (LO) of the collinear parton model (CPM), where one retains $\mathcal{O}(\alpha_s\alpha_{em})$ terms, direct photons originate from two subprocesses: $q + g \to q + \gamma$ Compton scattering, which is strongly dominant, and quark–antiquark annihilation leading to the production of a photon and a gluon, $q + \bar{q} \to g + \gamma$, where, for $p_T \simeq 2$–6 GeV, $q = u, d, s$. The same processes are considered within the GPM approach used here. To date, calculations of the cross section for direct photon production within the CPM framework have been performed in the next-to-leading order (NLO) [39–41] and even in the next-to-next-to-leading order (NNLO) [42] of perturbative QCD. Within the GPM approach, however, the procedure for calculating higher order corrections in the strong coupling constant has not been validated theoretically, and they are included phenomenologically by introducing a K factor. One possible way to include higher order corrections in the GPM framework is to take into account the fragmentation production of photons. This corresponds to the leading-logarithm approximation at the NLO level. Since fragmentation photons are emitted primarily from quarks, the production of such photons is dominated by processes of quark–quark scattering. This enhances the contribution of the quark Sivers function to transverse single-spin asymmetries. The contribution of the fragmentation production mechanism can be suppressed substantially upon imposing conditions of cone isolation on photon production in inclusive processes [43]. Considering the production of isolated photons, one can guarantee the dominance of the contribution of the gluon Sivers function over the contribution of the quark one in the asymmetry being considered and restrict oneself to taking into account the contribution of direct photons exclusively in theoretical calculations.

In the LO approximation, the standard formula of CPM factorization of the differential cross section for direct photon production has the form

$$d\sigma_{\rm dir}^{\rm CPM} = \int dx_1 f_a(x_1,\mu^2) \times \int dx_2 f_b(x_2,\mu^2) d\hat{\sigma}(a(q_1)b(q_2) \to \gamma(p_\gamma)c), \quad (1)$$

$$d\hat{\sigma} = \frac{1}{16\pi^2 I}\frac{d^3p_{\gamma T}}{E_3} \times \overline{|\mathcal{M}(a(q_1)b(q_2) \to \gamma(p_\gamma)c)|^2}\,\delta(\hat{s}+\hat{t}+\hat{u}), \quad (2)$$

where $d\hat{\sigma}$ is the cross section for hard Compton scattering or annihilation; $I = 2x_1x_2S$ is the flux factor; $f_{a(b)}(x_{1,2},\mu^2)$ stand for the collinear distributions of partons $a(b)$ in the protons; x_1 and x_2 are the parton fractions of the longitudinal momentum of protons colliding at the energy of $\sqrt{S} = \sqrt{(P_1+P_2)^2}$ in their center-of-mass (c.m.) frame with momenta $P_1^\mu = \left(\frac{\sqrt{S}}{2},0,0,\frac{\sqrt{S}}{2}\right)$ and $P_2^\mu = \left(\frac{\sqrt{S}}{2},0,0,-\frac{\sqrt{S}}{2}\right)$ in the collinear approximation—that is, $q_i = x_iP_i$, $i = 1,2$; $\hat{s} = (q_1+q_2)^2$, $\hat{t} = (q_1-p_\gamma)^2$, and $\hat{u} = (q_2-p_\gamma)^2$ are the Mandelstam variables; $\overline{|\mathcal{M}(a(q_1)b(q_2) \to \gamma(p_\gamma)c)|^2}$ is the squared modulus of the amplitude for the hard parton-scattering process $a+b \to \gamma+c$; and $\mu = \mu_R = \mu_F$—we assume that the renormalization scale is identical to the factorization scale and discuss a specific choice of μ below.

The results of the LO calculations within the CPM framework fall substantially short of experimental data, and this is indicative of the need for taking into account NLO corrections [44], but, even upon the inclusion of the NLO contributions, the theoretical results underestimate the experimental data [45, 46]. At same time, the standard factorization scheme within the parton model and QCD disregards the motion of partons within initial hadrons, assuming that the parton momenta are collinear to the momenta of colliding hadrons. The GPM approach is a phenomenological extension of the CPM approach. Within this extension, one introduces parton distributions depending on the intrinsic transverse momentum ($\mathbf{q}_T$). This model was first proposed in [21] for unpolarized processes and was successfully used later on to describe single-spin asymmetries in inclusive production [47–49].

For a detailed description of the GPM formalism, we refer the interested reader to [50]. Here, we give a succinct account of the formulas necessary for our calculations.

Within the GPM approach, the initial transverse momenta of partons, $q^\mu_{1(2)T}$, are included in the total 4-momentum of partons, $q^\mu_{1(2)}$, in a way that ensures their on-shell character ($q_1^2 = q_2^2 = 0$); that is,

$$q_1^\mu = x_1\frac{\sqrt{S}}{2}\left(1+\frac{q_{1T}^2}{x_1^2S},\mathbf{q}_{1T},1-\frac{q_{1T}^2}{x_1^2S}\right), \quad (3)$$

$$q_2^\mu = x_2\frac{\sqrt{S}}{2}\left(1+\frac{q_{2T}^2}{x_2^2S}, \mathbf{q}_{2T}, -1+\frac{q_{2T}^2}{x_2^2S}\right). \quad (4)$$

According to the GPM approach, the invariant differential cross section for direct photon production in the process $pp \to \gamma X$ is factorized in the form

$$d\sigma_{\rm dir}^{\rm GPM} \quad (5)$$
$$= \sum_{a,b}\int dx_1 d^2\mathbf{q}_{1T}\Phi_a(x_1,\mathbf{q}_{1T},\mu^2)$$
$$\times \int dx_2 d^2\mathbf{q}_{2T}\Phi_b(x_2,\mathbf{q}_{2T},\mu^2)$$
$$\times d\hat{\sigma}(a(q_1)b(q_2)\to\gamma(p_\gamma)c),$$

where $a, b = q, \bar{q}, g$, while $d\hat{\sigma}$ is given by an expression that is similar to expression (2). After some algebra, expression (5) can be recast into the form

$$\frac{d\sigma_{\rm dir}^{\rm GPM}}{dp_{\gamma T}dy_\gamma} \quad (6)$$
$$= \frac{1}{8\pi}\sum_{a,b}\int dx_1 d^2\mathbf{q}_{1T}\Phi_a(x_1,\mathbf{q}_{1T},\mu^2)$$
$$\times \int dx_2 d^2\mathbf{q}_{2T}\Phi_b(x_2,\mathbf{q}_{2T},\mu^2)$$
$$\times \frac{p_{\gamma T}}{x_1x_2S}\overline{|\mathcal{M}(a(q_1)b(q_2)\to\gamma(p_\gamma)c)|^2}\,\delta(\hat{s}+\hat{t}+\hat{u}),$$

where y_γ is the photon rapidity and $p_{\gamma T}$ is the photon transverse momentum.

The dependence on the intrinsic transverse momentum in the parton distribution $\Phi_a(x_i,\mathbf{q}_{iT})$ is factorized and is specified in the form of a Gaussian distribution featuring a phenomenological parameter $\langle q_T^2\rangle$; that is,

$$\Phi_a(x,\mathbf{q}_T,\mu^2) = f_a(x,\mu^2)\frac{1}{\pi\langle q_T^2\rangle^{1/2}}e^{-q_T^2/\langle q_T^2\rangle}. \quad (7)$$

Various estimates can be found in the literature for the numerical value of this parameter. They depend on the experimental-data sets included in the fitting procedure. In the most self-consistent way, the value of this parameter was extracted in [51]. The result was $\langle q_{qT}^2\rangle = 0.25$ GeV^2 for quarks and $\langle q_{gT}^2\rangle = 1$ GeV^2 for gluons.

By employing these values and relying on the GPM approach, within which we took the CTEQ11 collinear parton distributions [52], we calculated the differential cross sections with respect to the transverse momentum for direct photon production in the PHENIX experiment reported in [53]. In order to take into account NLO corrections, we used a phenomenological K factor. The dependence of the K factor on the photon transverse momentum at the c.m. collision energies of $\sqrt{S} = 17.3$, 19.4, and 63 GeV was explored in [54]. The experimental data of the PHENIX Collaboration from [53] could be described within the GPM approach upon taking $K = 2.9$ at the central value of the hard scale $\mu = p_T$ (solid line). This is illustrated in Fig. 1, where the uncertainty associated with scale variations over the range of $p_T/2 < \mu < 2p_T$ is represented by the region shaded in gray.

3. TRANSVERSE SINGLE-SPIN ASYMMETRIES IN THE GENERALIZED PARTON MODEL

In the general form, the transverse single-spin asymmetry is given by the expression

$$A_N = \frac{d\sigma^\uparrow - d\sigma^\downarrow}{d\sigma^\uparrow + d\sigma^\downarrow}, \quad (8)$$

where the symbols $\uparrow$ and $\downarrow$ indicate opposite orientations of the proton spin that are orthogonal to the scattering plane in the c.m. frame of colliding protons.

For direct photons, we have

$$d\sigma^\uparrow - d\sigma^\downarrow = d\Delta\sigma \quad (9)$$
$$= \sum_{a,b=g,q,\bar{q}}\int dx_1 d^2\mathbf{q}_{1T}\int dx_2 d^2\mathbf{q}_{T2}$$
$$\times \Delta\Phi_{a/p^\uparrow}(x_1,\mathbf{q}_{1T},\mu^2)\Phi_{b/p}(x_2,\mathbf{q}_{2T},\mu^2)$$
$$\times \frac{p_{\gamma T}}{x_1x_2S}\overline{|\mathcal{M}(a(q_1)b(q_2)\to\gamma(p_\gamma)c)|^2}\,\delta(\hat{s}+\hat{t}+\hat{u}),$$

$$\Delta\Phi_{a/p^\uparrow}(x_1,\mathbf{q}_{1T},\mu^2) \quad (10)$$
$$\equiv \Phi_{a/p^\uparrow}(x_1,\mathbf{q}_{1T},\mu^2) - \Phi_{a/p^\downarrow}(x_1,\mathbf{q}_{1T},\mu^2)$$
$$= \Delta\Phi^N_{a/p^\uparrow}(x_1,q_{1T},\mu^2)\,\mathbf{S}\cdot(\hat{\mathbf{P}}\times\hat{\mathbf{q}}_{1T})$$
$$= \Delta\Phi^N_{a/p^\uparrow}(x_1,q_{1T},\mu^2)\cos\phi_a,$$

where $q_T = |\mathbf{q}_T|$, $\mathbf{q}_T = q_T(\cos\phi,\sin\phi)$; (x_1,q_{1T},μ^2) is the density of unpolarized partons $a = q, g$ that have an intrinsic transverse momentum $\mathbf{q}_{1T}$ within a transversely polarized proton $p^\uparrow$ whose 3-momentum and spin vector are denoted by $\mathbf{P}$ and $\mathbf{S}$, respectively; $\hat{\mathbf{P}} = \mathbf{P}/|\mathbf{P}|$ and $\hat{\mathbf{q}}_T = \mathbf{q}_T/|\mathbf{q}_T|$ are unit vectors; $\Delta^N\Phi_{a/p^\uparrow}(x_1,q_{1T},\mu^2)$ is the Sivers function [55]; and $\Phi_{b/p}(x_2,\mathbf{q}_{2T},\mu^2)$ is the distribution of partons $b = q, g$ in an unpolarized proton. The parton b within a polarized proton may be both a quark (an antiquark) and a gluon; therefore, the total asymmetry associated with the Sivers function is in fact the sum of the asymmetries related to the quark and gluon Sivers functions: $A_N = A_N^q + A_N^g$.

The experimental data available at the present time permit extracting the quark Sivers function, but the

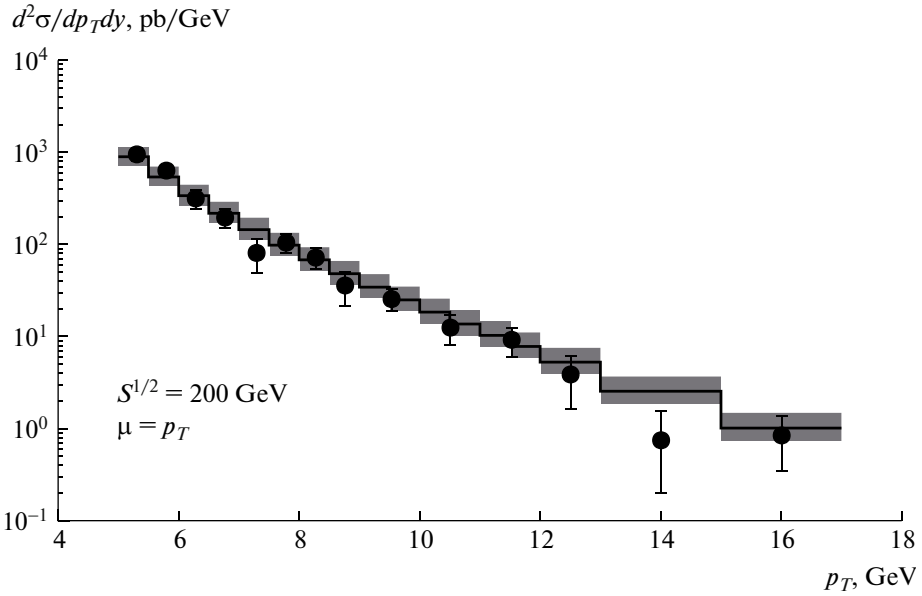

Fig. 1. Spectra of direct photon production at $\sqrt{S} = 200$ GeV. The solid line corresponds to our calculations within the GPM approach at $\mu = p_T$, the region shaded in gray reflects the uncertainty that arises upon varying μ over the range of $p_T/2 < \mu < 2p_T$, and the points represent experimental data of the PHENIX Collaboration [53].

gluon Sivers function has not yet received adequate study. An indirect estimations of the gluon Sivers function was performed within the GPM approach in [56], where this function was fitted to data on the single-spin asymmetry in neutral-pion production at the Relativistic Heavy Ion Collider (RHIC) in the central rapidity region. A calculation of transverse asymmetries that arise in direct photon production at the RHIC energies ($\sqrt{S} = 200$ GeV) and which may owe their existence to the contribution of the gluon Sivers function was performed in [57] within the GPM approach and within its color gauge-invariant extension.

The Sivers function admits different functional parametrizations. Here, we make use of the parametrization from the article of D'Alesio and his coauthors [56], who presented parameter sets for the gluon Sivers function; that is,

$$\Delta\Phi^N_{a/p^\uparrow}(x, q_T, \mu^2) \tag{11}$$
$$= 2\mathcal{N}_a(x) f_{a/p}(x, \mu^2) h(q_T) \frac{e^{-q_T^2/\langle q_T^2\rangle}}{\pi\langle q_T^2\rangle},$$

$$\mathcal{N}_a(x) = N_a x^{\alpha_a}(1-x)^{\beta_a} \frac{(\alpha_a+\beta_a)^{\alpha_a+\beta_a}}{\alpha_a^{\alpha_a}\beta_a^{\beta_a}}, \tag{12}$$

$$h(q_T) = \sqrt{2e}\frac{q_T}{M} e^{-q_T^2/M^2}, \tag{13}$$

where $|N_a| \le 1$. Following [56], one can introduce the parameter $\rho = \dfrac{M^2}{\langle q_T^2\rangle + M^2}$ for the gluon Sivers function, whereupon expression (11) assumes the form

$$\Delta\Phi^N_{g/p^\uparrow}(x, q_T, \mu^2) = 2\mathcal{N}_g(x) f_{a/p}(x, \mu^2) \tag{14}$$
$$\times \frac{\sqrt{2e}}{\pi}\frac{\sqrt{1-\rho}}{\rho} q_T \frac{e^{-q_T^2/\rho\langle q_T^2\rangle}}{\langle q_T^2\rangle^{3/2}}.$$

A saturated Sivers function for which one takes the values of $\mathcal{N}_a(x) = 1$ and $\rho = 2/3$ is the simplest parametrization [58], which permits estimating maximum possible asymmetries and relative contributions of quarks and gluons. The calculations performed with the saturated Sivers function lead to asymmetry values ranging between 4% and 6% and exceeding substantially existing experimental data. In the following, we therefore do not use this parametrization.

In the present study, we consider three versions of the choice of parameters for the Sivers function. The parameters of the quark Sivers function that were extracted from a fit to the experimental data measured by the HERMES and COMPASS Collaborations for transverse single-spin azimuthal asymmetries in the production of charged hadrons [59] and in processes of semi-inclusive deep-inelastic scattering (DIS) for transverse single-spin azimuthal asymmetries in pion and kaon production with allowance for the u, d, and s quark flavors [60], together with the parameters of the gluon Sivers function that were determined from the best fit in [56] for either parametrization of the quark Sivers function, will be referred to as, respectively, the SIDIS1 and SIDIS2 parameter sets. The parameters of the quark Sivers function that are identical to those

in the SIDIS1 set, together with the parameters of the gluon Sivers function that were extracted in the article of D'Alesio and his coauthors [51], will be denoted by D2019. The values of these parameters, together with the values of the parameter $\langle q_T^2\rangle$ in expression (7), are listed in Tables 1 and 2 for, respectively, the quark and gluon parametrizations.

4. FORMALISM OF THE COLOR GAUGE-INVARIANT EXTENSION OF THE GENERALIZED PARTON MODEL

The quark Sivers function extracted from experimental data on semi-inclusive DIS can be used to describe asymmetries in hadron–hadron collisions since the hypothesis of a universal character of the dependence on the intrinsic transverse momentum of parton distributions is adopted within the GPM framework. This means that effects of ISI and FSI between structure partons and soft spectator residues of the polarized proton are disregarded in the total scattering amplitude, as is illustrated in Fig. 2*a*. The ISI and FSI effects may be different in different scattering processes: by way of example, we indicate that, in semi-inclusive DIS, the quark produced in the parton-scattering process may exchange soft gluons with proton residues, which is FSI, while, in the Drell–Yan process, a quark from the unpolarized proton may exchange soft gluons with the transversely polarized proton, initiating ISI. Color states generated by these interactions may complicate substantially the color structure of the Sivers function in proton–proton interactions since both ISI and FSI effects are present in them [61], giving rise to the dependence of the Sivers function on the scattering process. A GPM extension in the form of the color gauge-invariant generalized parton model (CGI GPM) [23–25] was proposed in order to take this dependence into account. Within the CGI GPM approach, the process dependence of the quark Sivers function is considered in the one-gluon-exchange approximation, which permits absorbing this dependence in the parton cross sections, but leaves the the Sivers function universal. The Feynman diagrams illustrating ISI and FSI in the one-gluon approximation for photon production in $p^\uparrow p\to\gamma X$ processes are depicted in Figs. 2*b* and 2*c*, respectively. The modified parton production cross sections have the same form in terms of the Mandelstam variables as the hard twist-3 functions of the collinear approach [23].

In the formulas given below and associated with the CGI GPM approach, we will make use of a different definition of the Sivers function, $\Phi_{1T}^{\perp q}(x_i,q_{Ti},\mu^2)$. It is related to $\Delta^N\Phi_{q/p^\uparrow}(x_i,q_{Ti},\mu^2)$ by the equation

$$\Delta^N\Phi_{q/p^\uparrow}(x,q_T,\mu^2)=-\frac{q_T}{M}\Phi_{1T}^{\perp q}(x,q_T,\mu^2). \quad (15)$$

In order to take into account the process dependence of the quark Sivers function within the CGI GPM approach, it is then necessary to make the following substitution in expression (9):

$$\Phi_{1T}^{\perp q}\overline{|\mathcal{M}(qb\to\gamma c)|^2}\equiv\Phi_{1T}^{\perp q}\sum_{i,j}\mathcal{A}_i\mathcal{A}_j^* \quad (16)$$

$$\to\Phi_{1T}^{\perp qb\to\gamma c}\sum_{i,j}\mathcal{A}_i\mathcal{A}_j^*=\frac{C_I^{ij}+C_{F_c}^{ij}}{C_U^{ij}}\Phi_{1T}^{\perp q}$$

$$\times\sum_{i,j}\mathcal{A}_i\mathcal{A}_j^*\equiv\Phi_{1T}^{\perp q}\overline{|\mathcal{M}(qb\to\gamma c)|^2}^{\mathrm{CGI}}.$$

Here, the indices run through all diagrams contributing to the parton process being considered; C_U^{ij} is the color factor appearing in $\overline{|\mathcal{M}(qb\to\gamma c)|^2}$ in the unpolarized case; and C_I^{ij} and $C_{F_c}^{ij}$ are the color factors arising upon the summation of, respectively, ISI and FSI for each of the diagrams.

Within the CGI GPM approach, the gluon Sivers function is represented as a linear combination of two independent and universal gluon distributions $\Phi_{1T}^{\perp g(f)}$ and $\Phi_{1T}^{\perp g(d)}$ with coefficients that are calculated for each parton process. Two different gluon Sivers distributions correspond to two possible ways of formation of color-singlet combinations in three-gluon vertex functions via a convolution with a symmetric ($T_{bc}^a\equiv -if_{abc}$) or an antisymmetric ($D_{bc}^a\equiv d_{abc}$) constant of the $SU(3)$ color group; that is,

$$\Phi_{1T}^{\perp g}\overline{|\mathcal{M}(gb\to\gamma c)|^2}_U\equiv\Phi_{1T}^{\perp g}\sum_{i,j}\mathcal{A}_i\mathcal{A}_j^* \quad (17)$$

$$\to\Phi_{1T}^{\perp gb\to cd}\sum_{i,j}\mathcal{A}_i\mathcal{A}_j^*$$

$$\equiv\left(\Phi_{1T}^{(f)\perp gb\to cd}+\Phi_{1T}^{(d)\perp gb\to cd}\right)\sum_{i,j}\mathcal{A}_i\mathcal{A}_j^*$$

$$=\frac{C_I^{ij(f)}+C_{F_c}^{ij(f)}}{C_U^{ij}}\Phi_{1T}^{\perp g}\sum_{i,j}\mathcal{A}_i\mathcal{A}_j^*$$

$$+\frac{C_I^{ij(d)}+C_{F_c}^{ij(d)}}{C_U^{ij(d)}}\Phi_{1T}^{\perp g}\sum_{i,j}\mathcal{A}_i\mathcal{A}_j^*$$

$$\equiv\Phi_{1T}^{\perp g(f)}\overline{|\mathcal{M}(gb\to\gamma c)|^2}_{\mathrm{CGI}(f)}$$

$$+\Phi_{1T}^{\perp g(d)}\overline{|\mathcal{M}(gb\to\gamma c)|^2}_{\mathrm{CGI}(d)}.$$

A detailed discussion of ISI and FSI effects, together with the illustrations of one-gluon-exchange diagrams, as well as a complete set of formulas for hard parton processes with color factors in the CGI GPM approach, can be found in [23, 57]. Presented

Table 1. Parameter sets for the quark Sivers function

Name	N_u	$N_{\bar{u}}$	N_d	$N_{\bar{d}}$	N_s	$N_{\bar{s}}$	α_u	α_d	$\alpha_{\rm sea}$	β_u	β_d	M^2, $(\mathrm{GeV}/c)^2$	$\langle q_T^2\rangle$, $(\mathrm{GeV}/c)^2$
SIDIS1	0.32		−1.00				0.29	1.16		0.53	3.77	0.32	0.25
SIDIS2	0.35	0.04	−0.90	−0.40	−0.24	1.00	0.73	1.08	0.79	3.46	3.46	0.34	0.25
D2019	0.32		−1.00				0.29	1.16		0.53	3.77	0.32	0.25

below are only the equations that correspond to direct photon production. Specifically, we have

$$\overline{|\mathcal{M}(qg\to\gamma q)|^2}_U = -16\pi^2\alpha\alpha_s\frac{e_q^2}{N_c}\left(\frac{\hat{t}}{\hat{s}}+\frac{\hat{s}}{\hat{t}}\right), \tag{18}$$

$$\overline{|\mathcal{M}(qg\to\gamma q)|^2}_{\rm CGI} = -\overline{|\mathcal{M}(\bar{q}g\to\gamma\bar{q})|^2}_{\rm CGI} = 16\pi^2\alpha\alpha_s\frac{N_c}{N_c^2-1}e_q^2\left(\frac{\hat{t}}{\hat{s}}+\frac{\hat{s}}{\hat{t}}\right), \tag{19}$$

$$\overline{|\mathcal{M}(q\bar{q}\to\gamma g)|^2}_U = 16\pi^2\alpha\alpha_s\frac{N_c^2-1}{N_c^2}e_q^2\left(\frac{\hat{u}}{\hat{t}}+\frac{\hat{t}}{\hat{u}}\right), \tag{20}$$

$$\overline{|\mathcal{M}(q\bar{q}\to\gamma g)|^2}_{\rm CGI} = -\overline{|\mathcal{M}(\bar{q}q\to\gamma g)|^2}_{\rm CGI} = 16\pi^2\alpha\alpha_s\frac{e_q^2}{N_c^2}\left(\frac{\hat{u}}{\hat{t}}+\frac{\hat{t}}{\hat{u}}\right), \tag{21}$$

$$\overline{|\mathcal{M}(gq\to\gamma q)|^2}_U = -16\pi^2\alpha\alpha_s\frac{e_q^2}{N_c}\left(\frac{\hat{u}}{\hat{s}}+\frac{\hat{s}}{\hat{u}}\right), \tag{22}$$

$$\overline{|\mathcal{M}(gq\to\gamma q)|^2}_{\rm CGI(f)} = \overline{|\mathcal{M}(g\bar{q}\to\gamma\bar{q})|^2}_{\rm CGI(f)} = -\frac{1}{2}\overline{|\mathcal{M}(gq\to\gamma q)|^2}_U, \tag{23}$$

$$\overline{|\mathcal{M}(gq\to\gamma q)|^2}_{\rm CGI(d)} = -\overline{|\mathcal{M}(g\bar{q}\to\gamma\bar{q})|^2}_{\rm CGI(d)} = \frac{1}{2}\overline{|\mathcal{M}(gq\to\gamma q)|^2}_U. \tag{24}$$

Table 2. Parameter sets for the gluon Sivers function

Name	N_g	α_g	β_g	ρ	$\langle q_T^2\rangle$, $(\mathrm{GeV}/c)^2$
SIDIS1	0.65	2.8	2.8	0.687	0.25
SIDIS2	0.05	0.8	1.4	0.576	0.25
D2019	0.25	0.6	0.6	0.100	1.00

5. RESULTS OF CALCULATIONS

The results obtained by experimentally measuring single-spin asymmetries in direct photon production at the RHIC energy of $\sqrt{S}=200$ GeV in the central pseudorapidity region of $-0.35<\eta<0.35$ were recently published in [62]. In Fig. 3, the results of our calculations performed on the basis of the GPM approach with the SIDIS1, SIDIS2, and D2019 parameter sets are given along with the experimental data. Figure 3 shows that, for all parameter sets chosen in the present study, the theoretical results in question describe the experimental data within the errors everywhere, with the exception of one point in the region of low transverse momenta.

Figure 4 illustrates the predictions that we obtained within the GPM framework for the transverse asymmetries generated by the gluon and quark Sivers functions at $(a)\ \sqrt{S}=27$ GeV and $(b)\ \sqrt{S}=20$ GeV, employing the SIDIS1 parameter set. These results are given as a function of the Feynman variable $x_{\rm F}$ for the photon transverse momenta in the range of $4<p_T<6$ GeV. The solid and dashed lines represent the contributions of, respectively, the quark and gluon Sivers functions at the central choice of the hard scale, $\mu=p_T$. In the figures, the dependence of the predictions on this scale is shown by the dotted lines representing the boundaries of the corridor $p_T/2<\mu=2p_T$. Both for the gluon Sivers function and for the quark Sivers function, the uncertainties associated with the choice of value for the hard scale are obviously insignificant.

The dependences presented here show that, in the region of $x_{\rm F}<-0.2$, the contribution of the gluon Sivers function is the most distinct and increases monotonically as $x_{\rm F}$ decreases. By studying the region of $x_{\rm F}\lesssim-0.5$, we can therefore estimate directly the gluon Sivers function, but the resulting estimate would lie within the experimentally accessible region of $x_{\rm F}$ exclusively.

In Fig. 5, the above dependences are shown for the SIDIS2 and D2019 sets of parameters of the Sivers function. The total contributions of the quark and gluon Sivers functions are given in Fig. 6 for various choices of parameters of the Sivers function.

We can see that the largest asymmetry values are predicted upon choosing the SIDIS1 parameter

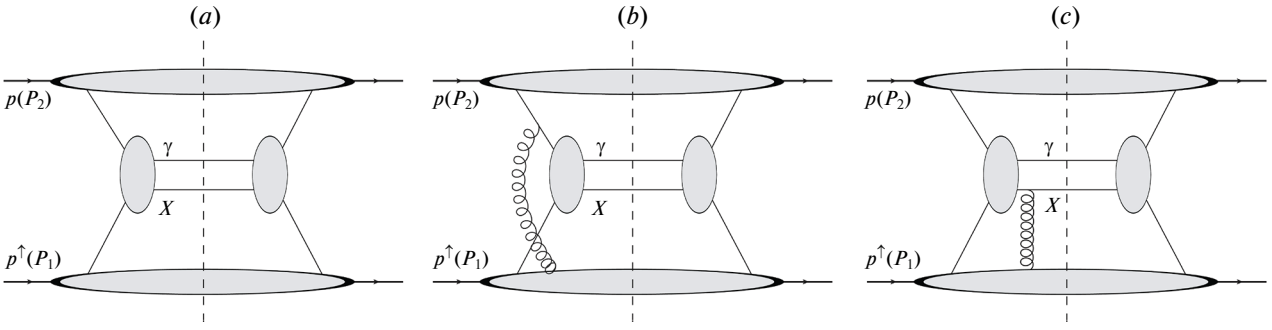

Fig. 2. Feynman diagrams corresponding to the process $p^{\uparrow}p \to \gamma X$ within the (a) GPM approach, (b) CGI GPM approach for the ISI case, and (c) CGI GPM approach for the FSI case.

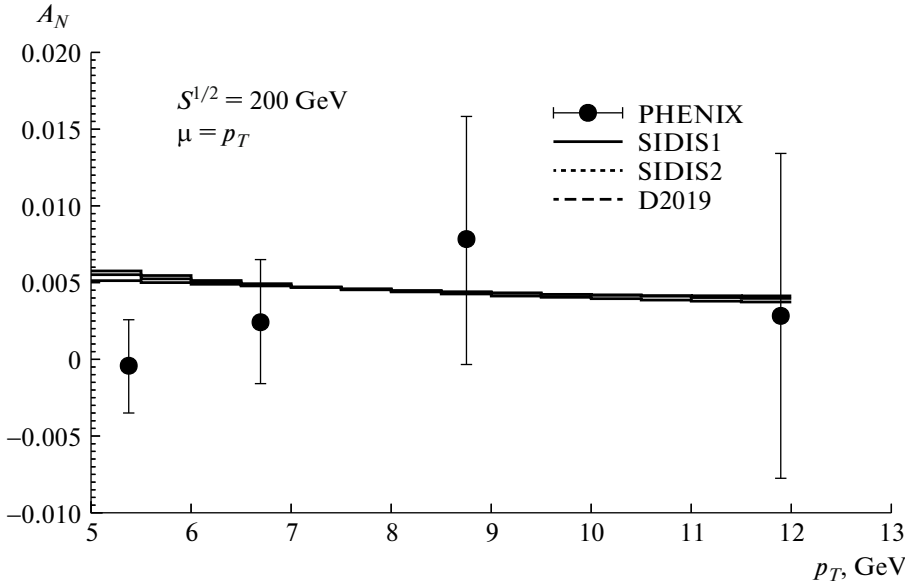

Fig. 3. Single-spin asymmetries in direct photon production at $\sqrt{S} = 200$ GeV. The solid, dotted, and dashed lines represent the results of our calculations based on the GPM approach and performed with, respectively, the SIDIS1, SIDIS2, and D2019 parameter sets, while the points on display stand for experimental data of the PHENIX Collaboration [62].

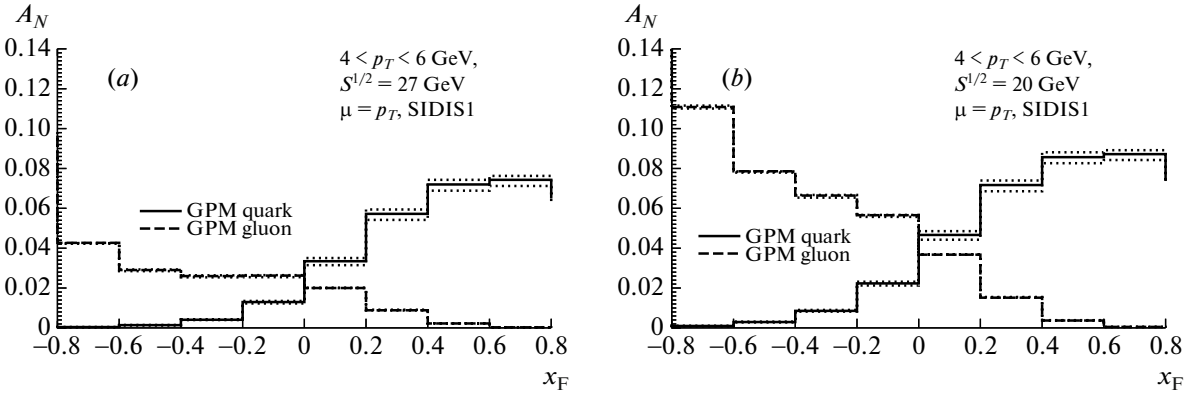

Fig. 4. Dependences of the contributions of the gluon and quark Sivers functions on x_F for $4 < p_T < 6$ GeV at (a) $\sqrt{S} = 27$ GeV and (b) $\sqrt{S} = 20$ GeV for the SIDIS1 parameter set [59].

set. The smallest asymmetry values are predicted in the case of choosing the SIDIS2 parameter set. At the absolute maximum, either contribution of the quark and gluon Sivers functions does not exceed 1.5%. The absolute values of the contribution of the gluon Sivers function decrease with increasing c.m. energy, but the problem of separation of background processes from signal ones complicates strongly the

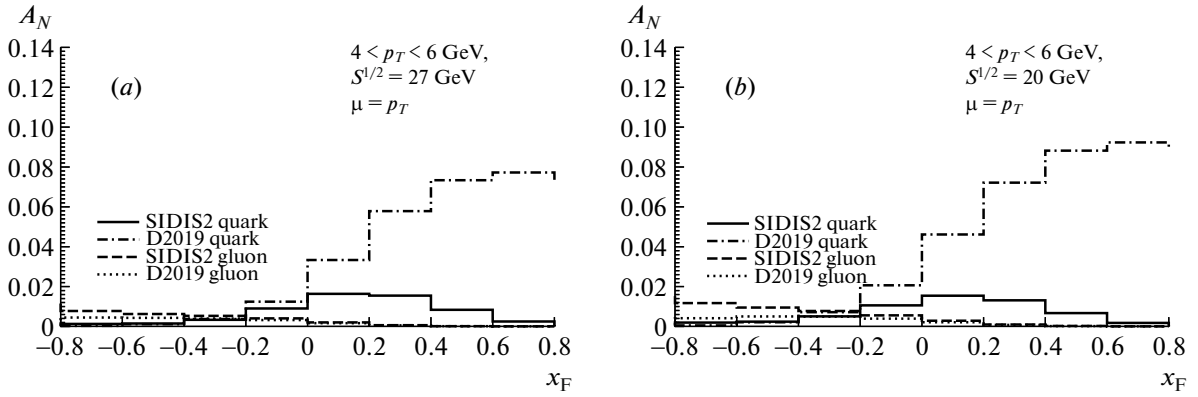

Fig. 5. Dependences of the contributions of the gluon and quark Sivers functions on x_F for $4 < p_T < 6$ GeV at (a) $\sqrt{S} = 27$ GeV and (b) $\sqrt{S} = 20$ GeV for the SIDIS2 [60] and D2019 [51] parameter sets.

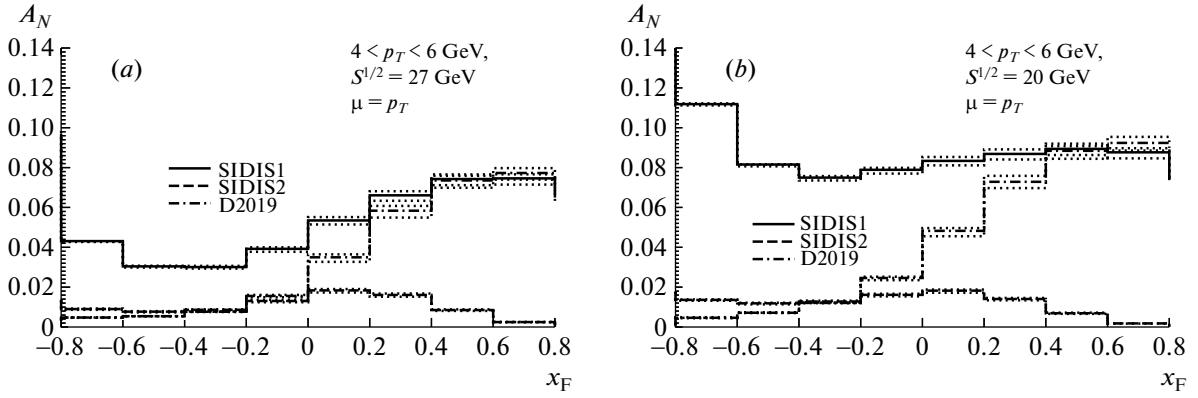

Fig. 6. Dependences of the total asymmetries on x_F for $4 < p_T < 6$ GeV at (a) $\sqrt{S} = 27$ GeV and (b) $\sqrt{S} = 20$ GeV for various choices of parameters for the Sivers function.

analysis of experimental data at relatively low energies of $\sqrt{S} < 20$ GeV. At the c.m. collisions energies of $\sqrt{S} = 20$ GeV and $\sqrt{S} = 27$ GeV, the GPM approach with the gluon Sivers function parameterized by employing the SIDIS1 set predicts 5% to 10% asymmetries, which admit experimental observations.

6. CGI GPR RESULTS

In Figs. 7, 8, and 9, the x_F dependences of the contributions associated with the d- and f-gluon Sivers functions and the quark Sivers function are given at (a) $\sqrt{S} = 27$ GeV and (b) $\sqrt{S} = 20$ GeV for, respectively, the SIDIS1, SIDIS2, and D2019 parameter sets. Since the d- and f-gluon Sivers functions are independent, their contributions can either form a sum or cancel each other; that is, the predicted asymmetry values, which one can observe experimentally, fall within the range from zero to the doubled absolute value of the contribution of the d-gluon (f-gluon) Sivers function. The quark Sivers function–induced asymmetries the within the CGI GPM approach are identical in magnitude to their counterparts within the GPM approach generalized parton model but are opposite to them in sign.

7. CONCLUSIONS

We have calculated transverse single-spin asymmetries in the production of direct photons in $p^{\uparrow}p$ collisions at the NICA energies of $\sqrt{S} = 20$ GeV and $\sqrt{S} = 27$ GeV, relying on the approach developed within the GPM framework on the basis of the hypothesis that transverse-momentum-dependent quark and gluon Sivers functions exist both in this approach and in its color gauge-invariant extension. Within the GPM approach, we have successfully described the existing experimental data of the PHENIX Collaboration [53] on direct photon production, thereby confirming the viability of the model used.

We have determined the hierarchy of the contributions of the gluon and quark Sivers functions to

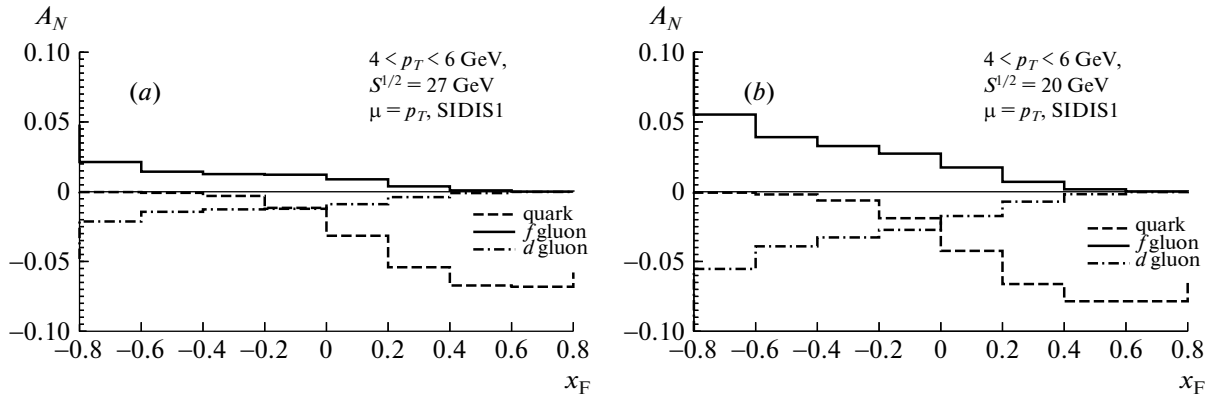

Fig. 7. Dependences of the contributions of the gluon and quark Sivers functions on x_F for $4 < p_T < 6$ GeV at (a) for $\sqrt{S} = 27$ GeV and (b) $\sqrt{S} = 20$ GeV for the SIDIS1 parameter set [59] in the CGI GPM approach.

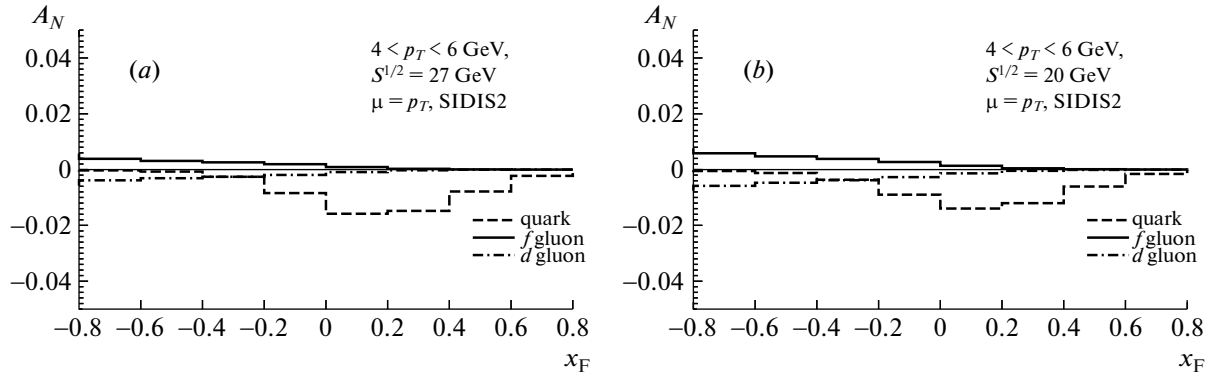

Fig. 8. As in Fig. 7, but for the SIDIS2 parameter set [60].

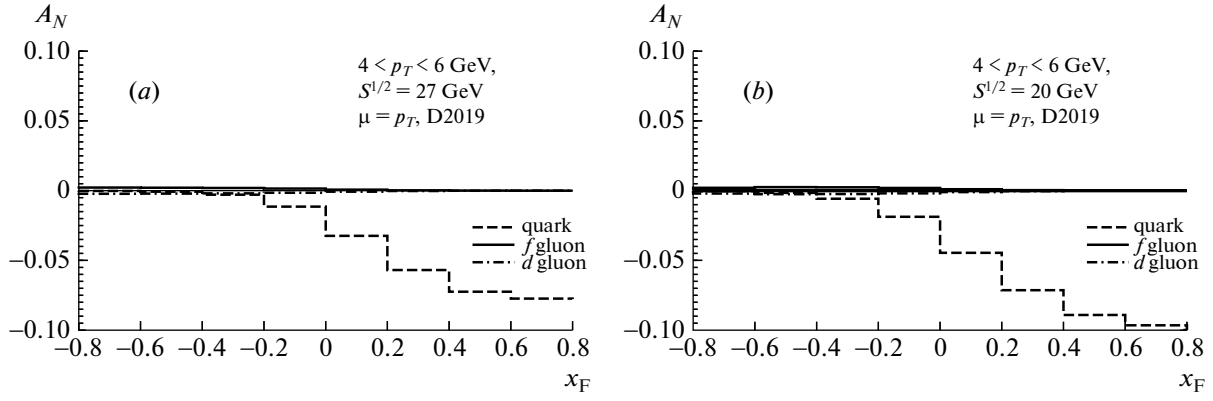

Fig. 9. As in Fig. 7, but for the D2019 parameter set [51].

the expected asymmetries and have singled out the region of $x_F < -0.4$ as that which is kinematically appropriate for extracting the gluon Sivers function in the case of implementation of a scenario that is favorable for its observation. We have considered three versions of parametrization of the Sivers functions and, among them, have singled out the SIDIS1 parameter set [59] as the most optimistic scenario for the observation of single-spin asymmetries induced by the gluon Sivers function. By employing this parametrization within both approaches—the GPM and CGI GPM ones—we have predicted the possibility of observing at a level of 10% down to 5% the gluon Sivers function–induced transverse asymmetries over the region of negative x_F values that is kinematically accessible to measurements and at the

NICA energies of $\sqrt{S} = 20$ GeV and $\sqrt{S} = 27$ GeV, which are the most promising for their observation. Within the CGI GPM approach, this estimate is valid in the case where the contributions of the d- and f-gluon Sivers functions are of the same sign. As was earlier indicated in [57], we cannot rule out none of the above scenarios of the appearance of transverse asymmetries.

ACKNOWLEDGMENTS

We are grateful to A. Gus'kov, I. Denisenko, O.Teryaev and other members of the SPD NICA Collaboration for enlightening comments and stimulating discussions.

FUNDING

This work was performed partly within fulfillment of the State Assignment of the Ministry of Science and Higher Education of Russian Federation for educational and research universities (project no. FSSS-2020-0014).

REFERENCES

1. D. Sivers, Phys. Rev. D **41**, 83 (1990).
2. D. Boer and P. J. Mulders, Phys. Rev. D **57**, 5780 (1998).
3. P. J. Mulders and R. D. Tangerman, Nucl. Phys. B **461**, 197 (1996).
4. A. Bacchetta, U. D'Alesio, M. Diehl, and C. Andy Miller, Phys. Rev. D **70**, 117504 (2004).
5. A. Bacchetta and M. Radici, Phys. Rev. Lett. **107**, 212001 (2011).
6. V. Barone, F. Bradamante, and A. Martin, Prog. Part. Nucl. Phys. **65**, 267 (2010).
7. M. G. Perdekamp and F. Yuan, Ann. Rev. Nucl. Part. Sci. **65**, 429 (2015).
8. E. C. Aschenauer, U. D'Alesio, and F. Murgia, Eur. Phys. J. A **52**, 156 (2016).
9. U. D'Alesio and F. Murgia, Prog. Part. Nucl. Phys. **61**, 394 (2008).
10. A. Arbuzov, A. Bacchetta, M. Butenschoen, F. G. Celiberto, U. D'Alesio, M. Deka, I. Denisenko, M. G. Echevarria, A. Efremov, N. Ya. Ivanov, A. Guskov, A. Karpishkov, Ya. Klopot, B. A. Kniehl, A. Kotzinian, S. Kumano, et al., Prog. Part. Nucl. Phys. **119**, 103858 (2021).
11. A. V. Efremov and O. V. Teryaev, Sov. J. Nucl. Phys. **36**, 140 (1982).
12. C. Kouvaris, J.-W. Qiu, W. Vogelsang, and F. Yuan, Phys. Rev. D **74**, 114013 (2006).
13. H. Eguchi, Y. Koike, and K. Tanaka, Nucl. Phys. B **763**, 198 (2007).
14. Y. Koike and T. Tomita, Phys. Lett. B **675**, 181 (2009).
15. K. Kanazawa, Y. Koike, A. Metz, and D. Pitonyak, Phys. Rev. D **89**, 111501(R) (2014).
16. X. Ji, J.-P. Ma, and F. Yuan, Phys. Rev. D **71**, 034005 (2005).
17. S. J. Brodsky, D. S. Hwang, and I. Schmidt, Phys. Lett. B **530**, 99 (2002).
18. S. J. Brodsky, D. S. Hwang, and I. Schmidt, Nucl. Phys. B **642**, 344 (2002).
19. A. Bacchetta, M. Diehl, K. Goeke, A. Metz, P. J. Mulders, and M. Schlegel, J. High Energy Phys. **0702**, 093 (2007).
20. D. Boer, P. J. Mulders, and F. Pijlman, Nucl. Phys. B **667**, 201 (2003).
21. R. P. Feynman, R. D. Field, and G. C. Fox, Phys. Rev. D **18**, 3320 (1978).
22. X. Ji, J.-P. Ma, and F. Yuan, Phys. Lett. B **597**, 299 (2004).
23. L. Gamberg and Z.-Bo Kang, Phys. Lett. B **696**, 109 (2011).
24. U. D'Alesio, L. Gamberg, Z.-Bo Kang, F. Murgia, and C. Pisano, Phys. Lett. B **704**, 637 (2011).
25. U. D'Alesio, F. Murgia, and C. Pisano, Phys. Part. Nucl. **45**, 110 (2014).
26. X. Ji, J.-W. Qiu, W. Vogelsang, and F. Yuan, Phys. Rev. Lett. **97**, 082002 (2006).
27. Y. Koike, W. Vogelsang, and F. Yuan, Phys. Lett. B **659**, 878 (2008).
28. A. Bacchetta, D. Boer, M. Diehl, and P. J. Mulders, J. High Energy Phys. **0808**, 023 (2008).
29. L. Gamberg and Z.-Bo Kang, Phys. Lett. B **718**, 181 (2012).
30. R. M. Godbole, A. Misra, A. Mukherjee, and V. S. Rawoot, Phys. Rev. D **85**, 094013 (2012).
31. R. M. Godbole, A. Kaushik, and A. Misra, Phys. Rev. D **94**, 114022 (2016).
32. R. M. Godbole, A. Kaushik, A. Misra, V. Rawoot, and B. Sonawane, Phys. Rev. D **96**, 096025 (2017).
33. R. M. Godbole, A. Kaushik, and A. Misra, Phys. Rev. D **97**, 076001 (2018).
34. S. Padval, R. M. Godbole, A. Kaushik, A. Misra, and V. S. Rawoot, Phys. Rev. D **103**, 036008 (2021).
35. M. Anselmino, M. Boglione, U. D'Alesio, E. Leader, S. Melis, and F. Murgia, Phys. Rev. D **73**, 014020 (2006).
36. M. Anselmino, M. Boglione, U. D'Alesio, E. Leader, S. Melis, F. Murgia, and A. Prokudin, Phys. Rev. D **86**, 074032 (2012).
37. M. Anselmino, M. Boglione, U. D'Alesio, S. Melis, F. Murgia, and A. Prokudin, Phys. Rev. D **88**, 054023 (2013).
38. D. Boer, C. Lorcé, C. Pisano, and J. Zhou, Adv. High Energy Phys. **2015**, 371396 (2015).
39. H. Baer, J. Ohnemus, and J. F. Owens, Phys. Rev. D **42**, 61 (1990).
40. L. E. Gordon and W. Vogelsang, Phys. Rev. D **50**, 1901 (1994).

41. M. Fontannaz, J. Ph. Guillet, and G. Heinrich, Eur. Phys. J. C **21**, 303 (2001).
42. X. Chen, T. Gehrmann, N. Glover, M. Höfer, and A. Huss, J. High Energy Phys. **2004**, 166 (2020).
43. S. Catani, M. Fontannaz, J. P. Guillet, and E. Pilon, J. High Energy Phys. **0205**, 028 (2002).
44. M. Glück, L. E. Gordon, E. Reya, and W. Vogelsang, Phys. Rev. Lett. **73**, 388 (1994).
45. X.-N. Wang, Phys. Rev. C **61**, 064910 (2000).
46. L. Apanasevich et al. (Fermilab E706 Collab.), Phys. Rev. Lett. **81**, 2642 (1998).
47. M. Anselmino and F. Murgia, Phys. Lett. B **442**, 470 (1998).
48. M. Boglione, U. D'Alesio, and F. Murgia, Phys. Rev. D **77**, 051502(R) (2008).
49. M. Anselmino, M. Boglione, U. D'Alesio, E. Leader, S. Melis, and F. Murgia, in *Proceedings of the 2nd International Workshop on Transverse Polarization Phenomena in Hard Processes (Transversity 2008), Ferrara, Italy, 2008,* Ed. by G. Ciullo, M. Contalbrigo, D. Hasch, and P. Lenisa (World Scientific, Singapore, 2009), p. 122.
50. U. D'Alesio and F. Murgia, Phys. Rev. D **70**, 074009 (2004).
51. U. D'Alesio, C. Flore, F. Murgia, C. Pisano, and P. Taels, Phys. Rev. D **99**, 036013 (2019).
52. J. Pumplin, D. R. Stump, J. Huston, H. L. Lai, P. Nadolsky, and W. K. Tung, J. High Energy Phys. **0207**, 012 (2002).
53. T. Sakaguchi (for the PHENIX Collab.), Acta Phys. Hung. A **25**, 409 (2006).
54. C.-Y. Wong and H. Wang, Phys. Rev. C **58**, 376 (1998).
55. S. M. Aybat, J. C. Collins, J. W. Qiu, and T. C. Rogers, Phys. Rev. D **85**, 034043 (2012).
56. U. D'Alesio, F. Murgia, and C. Pisano, J. High Energy Phys. **1509**, 119 (2015).
57. R. M. Godbole, A. Kaushik, A. Misra, and S. Padval, Phys. Rev. D **99**, 014003 (2019).
58. U. D'Alesio, F. Murgia, and C. Pisano, Phys. Rev. D **83**, 034021 (2011).
59. M. Anselmino, M. Boglione, U. D'Alesio, A. Kotzinian, F. Murgia, and A. Prokudin, Phys. Rev. D **72**, 094007 (2005).
60. M. Anselmino, M. Boglione, U. D'Alesio, A. Kotzinian, S. Melis, F. Murgia, A. Prokudin, and C. Türk, Eur. Phys. J. A **39**, 89 (2007).
61. A. Bacchetta, C. J. Bomhof, P. J. Mulders, and F. Pijlman, Phys. Rev. D **72**, 034030 (2005).
62. U. A. Acharya, C. Aidala, Y. Akiba, M. Alfred, V. Andrieux, N. Apadula, H. Asano, B. Azmoun, V. Babintsev, N. S. Bandara, K. N. Barish, S. Bathe, A. Bazilevsky, M. Beaumier, R. Belmont, A. Berdnikov, et al. (PHENIX Collab.), Phys. Rev. Lett. **127**, 162001 (2021).